Thevenin black box model to characterize conducted electromagnetic interference of DC/AC converters for aerospace applications

Noan Artaud, Jean-Marc Dienot, Isabelle Junqua, Laurent Guibert, Sara Boujouj

Thevenin black box model to characterize conducted electromagnetic interference of DC/AC converters for aerospace applications

Noan Artaud[#$], Jean-Marc Dienot[*$], Isabelle Junqua[#], Laurent Guibert[#], Sara Boujoujex[^]

[#]ONERA/DEMR, Université de Toulouse, France

[$]Laboratoire SIAME – Fédération IPRA EA4581, Université UPPA (Pau), France

[*]Labceem, Université Paul Sabatier – Toulouse III, France

[^]was with ONERA/DEMR, Université de Toulouse, France

{noan.artaud, isabelle.junqua, laurent.guibert}@onera.fr, jeanmarc.dienot@iut-tarbes.fr

***Abstract* — This article focuses on behavioral modelling of power systems, specifically DC/AC converters to evaluate electromagnetic (EM) interferences as conducted emissions current, at both inputs and outputs. A linear equivalent model of the converter is proposed as a five-port black box model, which allows for interaction between the input and output ports. To implement it, we associated it with experimental setups for measuring impedance and currents in frequency domain. The experimental setup only provides the amplitude of the current, so three hypotheses were proposed to determine the phase shift between the currents. To validate our model, we compare the measurements and calculations of current in common mode in conducted emissions for these three hypotheses.**

***Keywords* — DC/AC converters, Power Electronics, Conducted electromagnetic emission, Thevenin block model.**

I. INTRODUCTION

With the growing electric motorization of vehicles, power electronics components are nowadays commonly integrated in embedded equipment. Increasing the performance of power electronic elements by improving the speed of commutation of internal components in ever smaller volumes can generate electromagnetic (EM) interference problems. Consequently, to fulfil EMC standards, as for example section 21 of the aeronautic equipment standard named RTCA DO-160 or EUROCAE ED14, it is necessary to control these EM interferences (EMI) [1].

In this context, during pre-design phase, having a numerical EMI model of power equipment such as converters would help to conceive acceptable electrical architectures and to take corrective actions to lower EMC conducted emissions, as for example filter at equipment input if required.

Two categories of EMI models can be found:

- Exhaustive models with high fidelity level which intend to consider all variables and interactions between elementary components and relevant characteristics to obtain a very detailed model of the equipment. They offer the advantage to model different operational point and commutations. However, they can be complex to build due to the difficulty of assessing the elements contributing to the source of EM emissions and due to confidentiality constraints [2].
- Behavioral models: they aimed at representing the equipment as a "black" box without considering its elementary components. The equipment is reduced to a source of noise which is experimentally characterized. Different approaches are proposed in the literature ([3][4]): The first ones named as terminated models are limited to the evaluation of EMI at input ports (or output ports) with fixed conditions of terminations conditions at output port (respectively input ports) ([5], [6]); The second one known as unterminated models intends to predict EMI both at input and output of the equipment regardless of loads.

The objective of the work presented here is to build a behavioral EMI model for DC/AC converters based on a Thevenin generator and to propose an experimental process to obtain the relevant characteristics of this model. This model will be implemented for a 5kW laboratory test bench including a DC/AC converter and a brushless motor which is described in Section II. Section III is dedicated to the building of the model, its assumptions, the technical barriers to remove and finally its validation.

II. BRUSHLESS TEST BENCH

Our 5kW laboratory test bench under study has been designed with commercial elements from electric bike technology assembling two brushless motors mounted on wheels coupled by a transmission belt system and powered through a DC/AC converter. This DC/AC converter named BMSWC for Brushless Motor Sinus Wave controller is itself connected to a 72V DC power supply through two Line Impedance Stabilization Network (LISN). The use of current clamps and LISNs is based on the DO-160 aerospace standard. The clamp is positioned as close as possible to the converter. The position of the converter and harnesses is not representative of the standard.[1]. The test bench is depicted in Fig. 1.

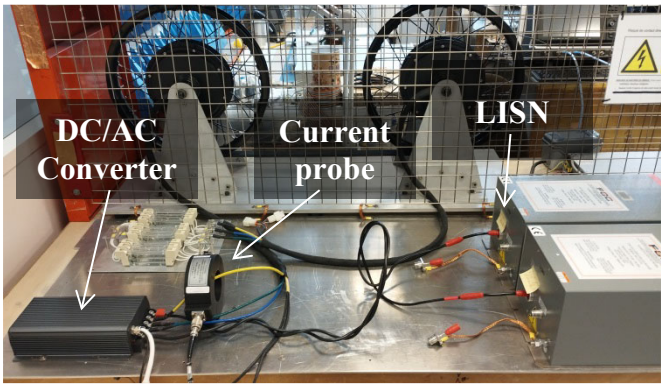

Fig. 1. Brushless Laboratory Test bench.

The corresponding block diagram is schemed in Fig. 2 where connections between the DC/AC converter inputs and the LISN in one side and between the DC/AC converter output and the motors on the other side are made through approximately 1m long cables.

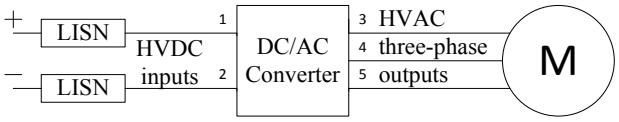

Fig. 2. Test bench Block diagram.

Measurements of the currents on port 1 and 2 on the DC side of the converter show switching signals. The damped sinusoidal waveforms are characteristic of transients, as shown in Fig. 3. Measurements of the functional currents at port 3, 4 and 5 on the AC side of the converter, which carry the power to the motor on the first, second and third phases respectively, are shown in Fig. 4. This recording was made using an oscilloscope that filters high frequencies. The three signals drove the motor at 220 Hz and had a characteristic phase shift of $2\pi/3$ between the three phases. Fig. 5 shows the current at port 3 of the converter measured with a high sampling frequency. The switching signals, potential sources of disturbance for the functional signal driving the motor, can be clearly seen.

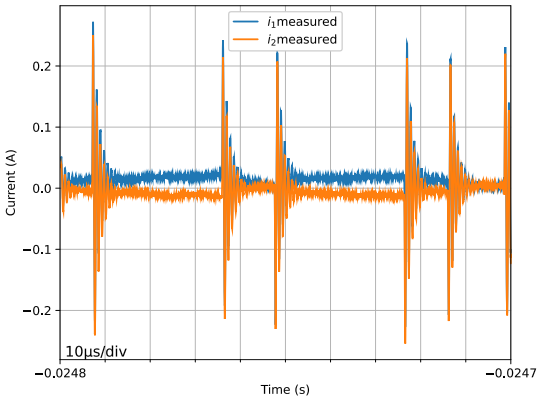

Fig. 3. DC side converter current measurement in time domain with a current probe connected to an oscilloscope

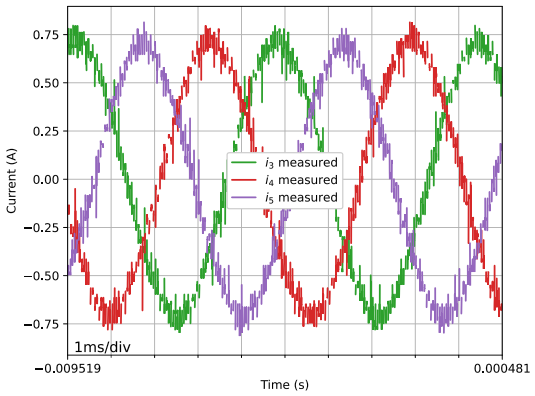

Fig. 4. AC side converter current measurement high frequency filtered. First, second and third line between the converter and the motor.

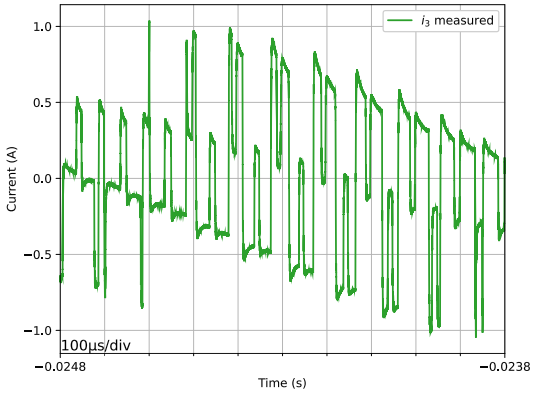

Fig. 5. AC side converter current measurement. First line between the converter and the motor.

III. Behavioral Model of the DC/AC Converter as a Thevenin Generator

A. Principles of a Thevenin Generator

A Thevenin generator is a simplified representation of a complex electrical circuit, characterized by an open-circuit voltage (E_{th}) and a Thevenin impedance (Z_{th}), enabling the analysis of interconnected circuits by replacing the original circuit with an equivalent.

The principle of Thevenin model can be generalized to a multiport system. In that case the Thevenin impedance is a matrix and the Thevenin voltage generator is a vector which dimensions are the number of ports of the system.

An assumption to apply Thevenin principles concerns source independence. An electrical circuit is considered independent when its sources of electrical energy, such as generators, do not rely on the currents or voltages in the rest of the circuit. This means that the characteristics of the Thevenin voltage generator remain constant regardless of the load elements of the circuit [8].

Furthermore, as we intend to implement a Thevenin model in frequency domain, it is necessary to fulfill the hypothesis of linearity [8]. However, a DC/AC converter relies on non-linear elements such as diodes and transistors. In [4], it has been demonstrated that if the impedance at the input ports is high enough, the contribution of non-linear elements is negligible. Consequently, it is possible to fulfill the conditions of linearity.

B. Experimental process to build the Thevenin generator model

To obtain the Thevenin model of the converter, it is necessary to determine the multiport voltage generator and its equivalent 5-port impedance matrix (see Fig. 6).

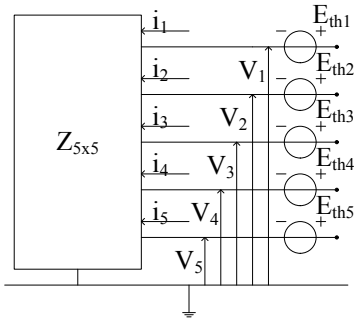

Fig. 6. Thevenin model of a five port circuit.

1) Thevenin Impedance

Measuring the impedance matrix non-intrusively and safely is a challenging task on a real-operating converter. In [9] (for frequencies above 150 kHz) and [10], it is demonstrated that measuring converter impedances in the 'OFF' mode is valid. This is explained by the fact that first stages of DC/AC converter are capacitances which "hide" in the frequency range under study the non-linear impedances of the operating converter [4].

Consequently the impedance matrix $[Z_{Conv}]$ of the converter can be deduced from classical scattering measurements $[S]$ of the non operating 5-ports system [10] as expressed in (1):

$$[Z_{Conv}] = ([Id] - [S])^{-1} . ([Id] + [S]) . [Zref]. \quad (1)$$

Where $[Id]$ is the identity matrix and $[Z_{ref}]$ is a reference impedance matrix on which the $[S]$ parameters are determined. In our case, $[S]$ parameters are measured over 50Ω with a vector network analyzer (VNA) and a full 2-ports calibration. When measuring S_{ij} ($1 \leqslant i \leqslant 5$, $1 \leqslant j \leqslant 5$), other converter ports k ($k \neq \{i,j\}$,) not connected to the VNA are loaded by 50 Ω .

Using the same process, impedances matrix of LISN and cables connected to the converter DC input on one side ($[Z_{LISN}]$), and motor and cables connected to the converter AC output on the other side ($[Z_{Motor}]$) were also extracted from S-parameters.(see Fig. 7)

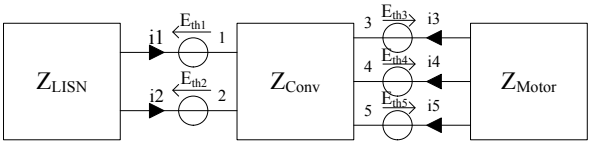

Fig. 7. Test bench Block-model

The analysis of resulting impedance is given in [7] and confirms that first stages of our DC/AC converter are capacitances.

2) Thevenin Voltage generator

Using the [Z] matrix of test bench elementary blocks and measured currents on each line of the converter loaded by LISN at its input and by the motor at its output, it is possible to derive the Thevenin voltage generator as in (2).

$$\begin{bmatrix} E_{th1} \\ E_{th2} \\ E_{th3} \\ E_{th4} \\ E_{th5} \end{bmatrix} = -[Z_{Loop}] * \begin{bmatrix} i_1 \\ i_2 \\ i_3 \\ i_4 \\ i_5 \end{bmatrix}. \quad (2)$$

Where $[Z_{Loop}]$ is the 5x5 matrix combining the three matrices of the circuit as in (3):

$$[Z_{Loop}] = \begin{bmatrix} [Z_{LISN}] & [0]_{2x3} \\ [0]_{3x2} & [0]_{3x3} \end{bmatrix} + [Z_{Conv}]_{5x5} + \begin{bmatrix} [0]_{2x2} & [0]_{2x3} \\ [0]_{3x2} & [Z_{Motor}] \end{bmatrix}. \quad (3)$$

Current on each branch was measured using a current probe connected to a spectrum analyzer (See Fig. 8.) from 1 kHz to 400 MHz. During the measurements, the engine power was set to a medium power of 2.5 kW.

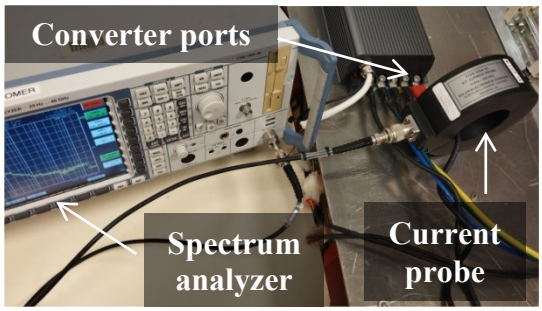

Fig. 8. Current measurement setup of the converter with a current probe connected to a spectrum analyzer

Fig. 9 shows currents measured at DC/AC converters ports. One can observe that EMI are larger at AC output than at DC input which can be explained by the fact that this converter is a Component Off The Shelf (COTS) with no filtering. These plots show EMI at 10 kHz, DC/AC converter switching frequency and at the following harmonics of 10 kHz. Around 1 MHz there is clearly broadband noise.

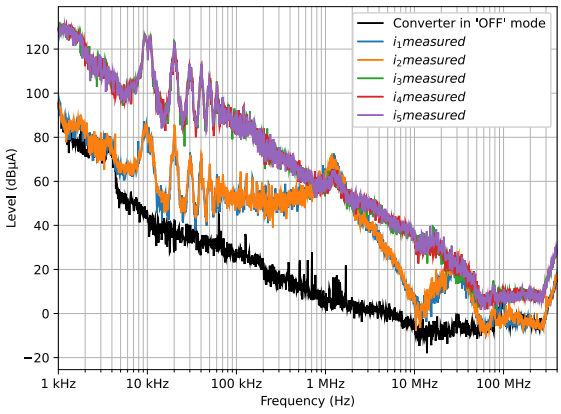

Fig. 9. Currents measured setup at DC/AC converter ports.

By conception, spectrum analyzers measure a power versus frequency, from which are deduced the magnitude of

the useful quantity, here the magnitude of the current once the transfer impedance of the current probe is taken into account. However, to calculate the Thevenin voltage generator vector as seen in (2), it is also necessary to have the phase shift between the 5 currents.

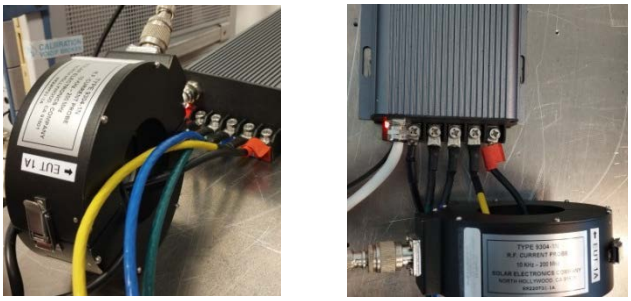

(a) (b)

Fig. 10. Current measurement mode: (a) Example of current subtraction measurement ; (b) Example of a current addition measurement

Three hypotheses were proposed to determine the phase shift between the currents.

- Hypothesis A: that there is no phase shift at all.
- Hypothesis B: i_1 and i_2 are in phase opposition, while output currents i_4 and i_5 are out of phase with i_3 by $2\pi/3$ and $4\pi/3$ respectively. This configuration consists in fact to apply the functional phase shift between the 5 branches of the DC/AC converter on the whole frequency range. Additionally, current i_1 and i_3 have no phase shift.
- Hypothesis C: the phase shift between currents i_k ($1 \leq k \leq 5$) are calculated from additional measurements of common mode and differential mode currents as illustrated in Fig. 10 and explained in Section C.3. In that case, there is no a priori restriction of fluctuation of phase shift versus frequency and no a priori correlation between functional signals and EMI signals.

Consequently, we obtain three sets of Thevenin model of the DC/AC converter.

C. Validation

To check the relevance of the three proposed hypotheses, we will compare the magnitude of common-mode currents (DC and AC sides of the converter) that were measured ($|i_1+i_2|$ and $|i_3+i_4+i_5|$) with those calculated using the three Thevenin's model as in (7) ($|i_1^{cal}+i_2^{cal}|$ and $|i_3^{cal}+i_4^{cal}+i_5^{cal}|$).

$$\begin{bmatrix} i_1^{cal} \\ i_2^{cal} \\ i_3^{cal} \\ i_4^{cal} \\ i_5^{cal} \end{bmatrix} = -([Z_{Loop}])^{-1} * \begin{bmatrix} E_{th1} \\ E_{th2} \\ E_{th3} \\ E_{th4} \\ E_{th5} \end{bmatrix} \quad (4)$$

Equations (2) and (4) being reciprocal, recalculation of currents on each of the DC/AC converter 5 ports would provide exactly the measured currents. Consequently comparing $|i_i|$ and $|i_i^{cal}|$ would not be a figure of merit.

1) Hypothesis A

In this configuration, there is no phase shift between measured currents at converter input and output ports. The resulting computed Thevenin voltage generators are displayed in Fig. 11 and shows similar magnitudes for the 5 ports.

Magnitudes of common mode currents on the DC side, as measured and calculated, have similar fluctuations. Nevertheless, at 10 kHz and at harmonics up to 50 kHz, the curves have an amplitude difference of more than 6 dB (see Fig. 12).

The amplitude of measured and calculated common mode currents on the AC side of the converter shows significant discrepancies in the whole frequency band except around 1MHz. (see Fig. 13).

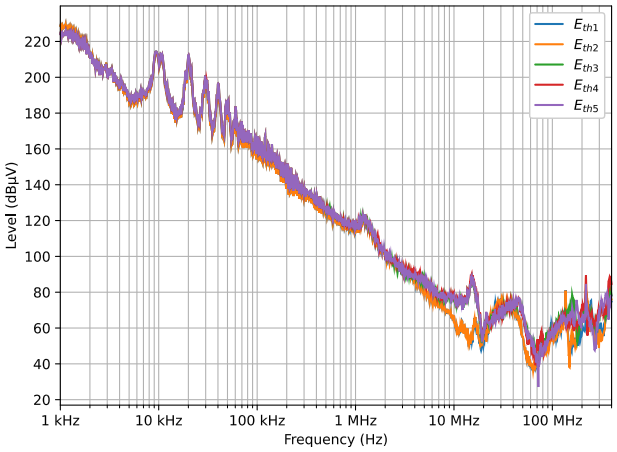

Fig. 11. Thevenin voltage generators

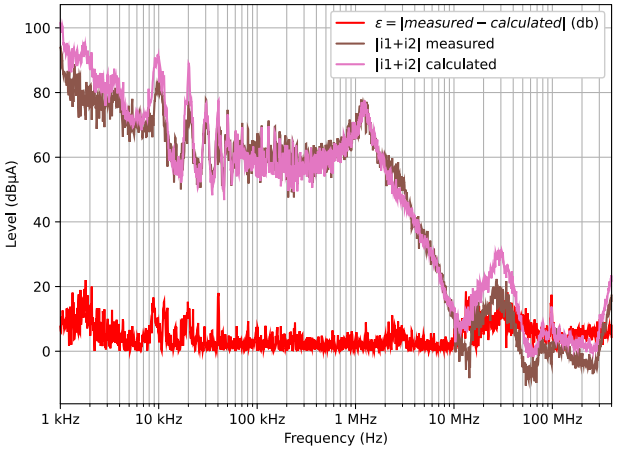

Fig. 12. Common mode current at DC input

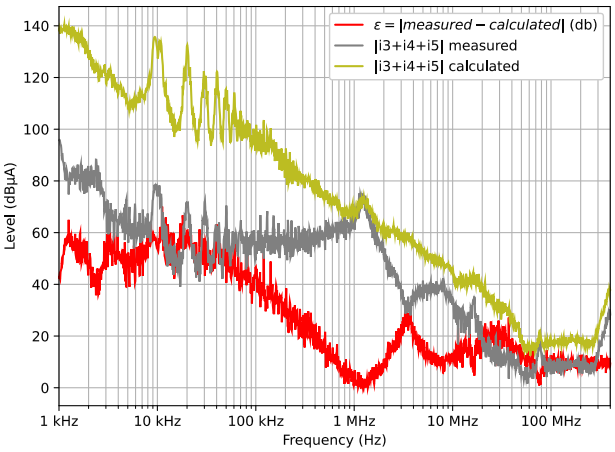

Fig. 13. Common mode current at AC output

2) Hypothesis B

Here, the hypothesis is that the DC side currents of the converter are in phase opposition, while the AC side currents are out of phase by an angle of $2\pi/3$. Thevenin generators plotted in Fig 15 follow the same trend as previously but are noisier. Calculation of the common mode current can lead to values tending towards zero, which in dB show large peaks.

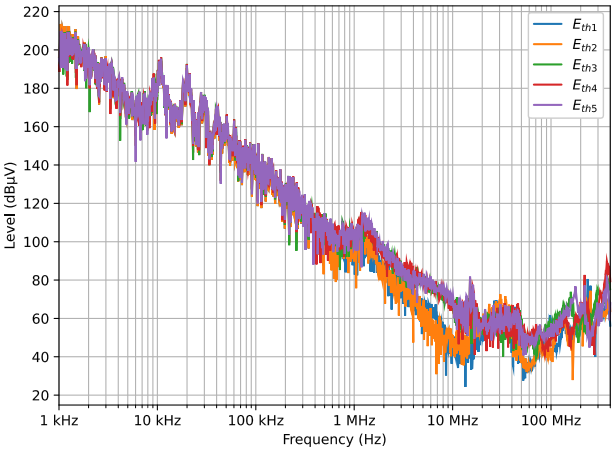

Fig. 14. Thevenin voltage generators

The measured and calculated common mode currents in Fig 16 on the DC side of the converter show deterioration in similarity. The relative error between amplitudes can reach 80 dB.

At low frequencies, the difference between the measured and calculated AC-side common-mode currents is smaller. Fig. 16 shows a relative error between amplitudes that is smaller than in the case without any phase shift, up to 40 dB.

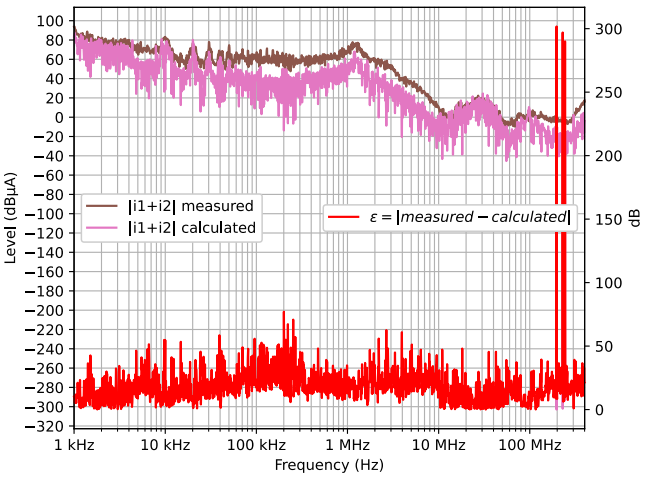

Fig. 15. Common mode current at DC input

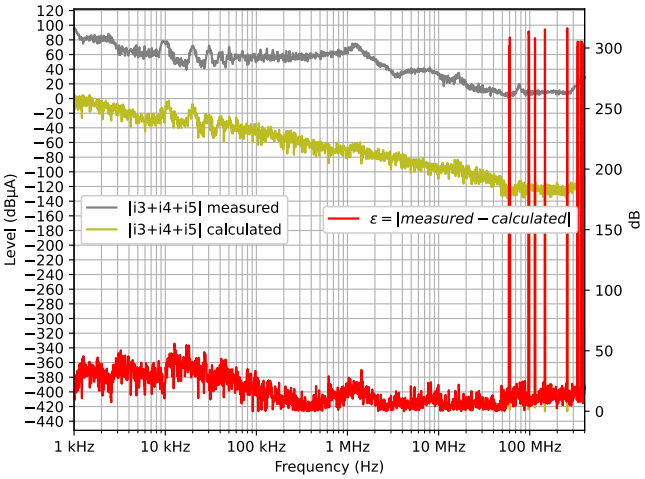

Fig. 16. Common mode current at AC output

3) Hypothesis C

Here the phase shift between i_1 and i_2, Φ_{21}, is calculated from the measurement of $|i_1+i_2|$ and $|i_1-i_2|$ (see Fig. 10a and Fig. 10b, as in (5)). The phase shift between currents at AC outputs, i_k ($k \in \{3, 4, 5\}$) and current i_1, Φ_{k1}, is calculated from the measurement of $|i_1+i_k|$ as in (6)).

$$\cos(\Phi_{21}) = \frac{|i_1 + i_2|^2 - |i_1 - i_2|^2}{4 * |i_1| * |i_2|} \quad (5)$$

$$\cos(\Phi_{k1}) = \frac{|i_1 + i_k|^2 - |i_1|^2 - |i_k|^2}{2 * |i_1| * |i_k|} \quad (6)$$

The common current measured and calculated on the DC side of the converter showed improved matching compared to the two previous configurations of phase shift.

However, there was no significant improvement in the common current on the AC side of the converter.

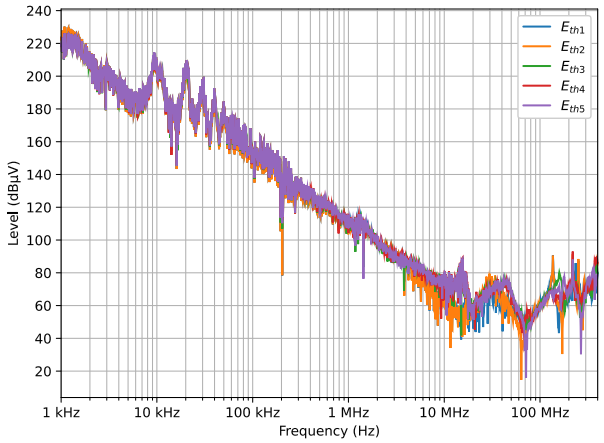

Fig. 17. Thevenin voltage generators

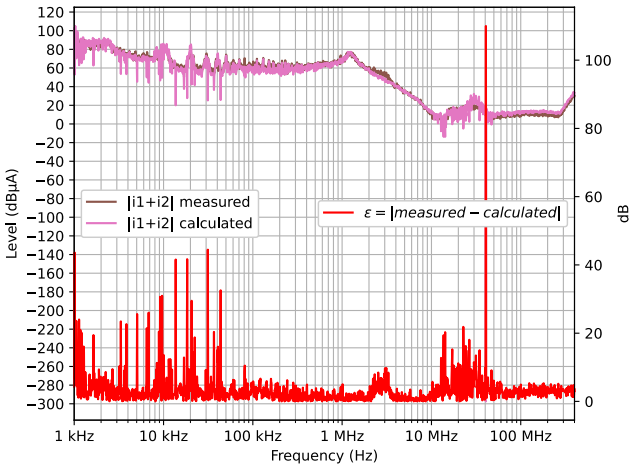

Fig. 18. Common mode current at DC input

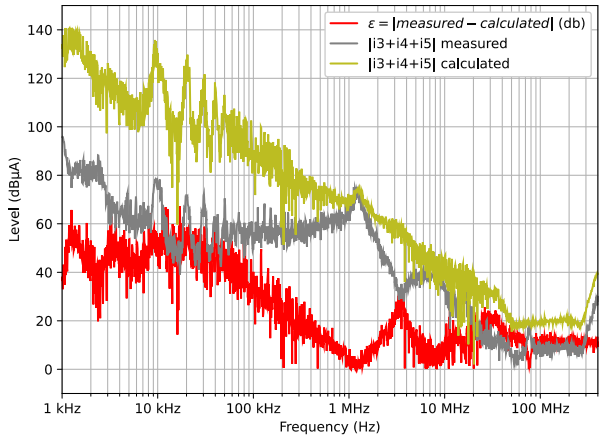

Fig. 19. Common mode current at AC output

IV. Conclusion

This paper presents a method to obtain the conducted EMI model of a DC/AC converter using a “black box” behavioral model based on Thevenin generator in frequency domain. It has been shown the importance to evaluate the phase shift between EMI interference in order to correctly reproduce common mode currents.

To improve this, as a prospect of this work, a digital algorithm can be used to minimize the error between the calculated and measured common-mode current. This approximation would provide valuable insights into the assumptions involved in determining the phase.

Additionally, using a multi-channel oscilloscope with a high sampling frequency can facilitate measuring currents and their phases. These measurements can then be transformed into the frequency domain using a Fourier transform. This method can be validated by comparing amplitude measurements with those obtained from a spectrum analyzer and the transformed currents.

Furthermore, using a vector network analyzer to measure the transfer of common-mode currents between the AC and DC sides of the converter, as well as between the differential mode and common mode, could also help to evaluate the behavioral model of the converter.

Acknowledgment

This work has been funded by the French DGAC in the PHYCIEL project (DGAC/DTA/SDC n° 2020-35), the Occitanie region (Emergence 23003066) and ONERA.

References

[1] RTCA DO-160G : Environmental Conditions and Test Procedures for Airborne Equipment, May , 2011, Prepared by SC-135, 2011 *RTCA Inc. available at https://do160.org/*

[2] A. R. Hefner, "An improved understanding for the transient operation of the power insulated gate bipolar transistor (IGBT)," in *IEEE Transactions on Power Electronics*, vol. 5, no. 4, pp. 459-468, Oct. 1990, doi: 10.1109/63.60690.

[3] M. Amara, “Control of conducted emissions of power electronics”, PHd Université de Lyon, 2019. In https://hal-lirmm.ccsd.cnrs.fr/AMPERE-THESE/tel-02500008v2

[4] H. Bishnoi, “Behavioral EMI Models of Switched Power Converters”, PHd Dr., 2013 also http://hdl.handle.net/10919/23936

[5] Q. Liu, F. Wang and D. Boroyevich, "Modular-Terminal-Behavioral (MTB) Model for Characterizing Switching Module Conducted EMI Generation in Converter Systems," in IEEE Transactions on Power Electronics, vol. 21, no. 6, pp. 1804-1814, Nov. 2006, doi: 10.1109

[6] M. Amara, C. Vollaire, M. Ali and F. Costa, "Black Box EMC Modeling of a Three Phase Inverter," 2018 International Symposium on Electromagnetic Compatibility, Amsterdam, Netherlands, 2018, pp. 642-647, doi: 10.1109/EMCEurope.2018.8485007

[7] L. Guibert, J-P. Parmantier, I. Junqua, M. Ridel. "Determination of Conducted EM Emissions on DC–AC Power Converters Based on Linear Equivalent Thevenin Block Circuit Models". IEEE Transactions on Electromagnetic Compatibility, 2021, 64 (1), pp.241-250

[8] O. Wing, Classical Circuit Theory. Boston, MA: Springer US, 2009. doi: 10.1007/978-0-387-09740-4.

[9] C. Cuellar, N. Idir, A. Benabou, and X. Margueron, ‘High frequency current probes for common-mode impedance measurements of power converters under operating conditions’, *EPE Journal*, vol. 24, no. 4, pp. 48–55, Dec. 2014, doi: 10.1080/09398368.2014.11755458.

[10] H. Jie, Z. Zhao, F. Fei, K. Y. See, R. Simanjorang, et F. Sasongko, « A Survey of Impedance Measurement Methods in Power Electronics », in 2022 IEEE International Instrumentation and Measurement Technology Conference (I2MTC), Ottawa, ON, Canada: IEEE, mai 2022, p. 1‑6. doi: 10.1109/I2MTC48687.2022.9806477.

[11] D. M. Pozar, *Microwave engineering*, Fourth Edition. Hoboken, NJ: John Wiley & Sons, Inc, 2012.

[12] L. Guibert, J-P. Parmantier, I. Junqua, “Analysis of EM conducted emissions on a three-phase HVDC/3HVAC power converter by a Thevenin model based method”, submitted to IEEE Transactions on Electromagnetic Compatibility